

ROSAT/ASCA OBSERVATIONS OF A SERENDIPITOUS BL LAC OBJECT PKS
2316-423: THE VARIABLE HIGH-ENERGY TAIL OF SYNCHROTRON RADIATIONSUI-JIAN XUE¹, YOU-HONG ZHANG²,

AND

JIAN-SHENG CHEN¹*To appear in The Astrophysical Journal, July 2000*

ABSTRACT

We present the analysis of archival data from ROSAT and ASCA of a serendipitous BL Lac object PKS 2316-423. Because of its featureless non-thermal radio/optical continuum, PKS 2316-423 has been called as a BL Lac candidate in the literature. PKS 2316-423 was evidently variable over the multiple X-ray observations, in particular, a variable high-energy tail of the synchrotron radiation is revealed. The X-ray spectral analysis provides further evidence of the synchrotron nature of its broad-band spectrum: a steep and downward curving spectrum between 0.1–10 keV, typical of high-energy peaked BL Lacs (HBL). The spectral energy distribution (SED) through radio-to-X-ray yields the synchrotron radiation peak at frequency $\nu_p = 7.3 \times 10^{15}$ Hz, with integrated luminosity of $L_{\text{syn}} = 2.1 \times 10^{44}$ ergs s⁻¹. The averaged SED properties of PKS 2316-423 are very similar to those “intermediate” BL Lac objects (IBL) found recently in several deep surveys, such as Deep X-ray Radio Blazar, Radio-Emitting X-ray, and ROSAT-Green Bank surveys. We suggest that PKS 2316-423 is an IBL though it also shows some general features of a HBL. Actually, this double attribute of PKS 2316-423 provides a good test of the prediction that an IBL object can show either synchrotron or inverse-Compton characteristics in different variability states.

keywords: BL Lac objects: individual (PKS 2316-423) – X-rays: galaxies

arXiv:astro-ph/0005422v1 22 May 2000

¹Beijing Astronomical Observatory and Beijing Astrophysics Center of National Astronomical Observatories, Chinese Academy of Sciences. A20 Datun Rd., Chaoyang District, Beijing 100012; E-mail: xue@bac.pku.edu.cn

²International School for Advanced Studies, SISSA/ISAS, via Beirut 2-4, I-34014 Trieste, Italy; E-mail: yhzhang@sissa.it

1. INTRODUCTION

BL Lac objects – a subclass of active galactic nuclei (AGN) – show variable non-thermal emissions from radio to UV/X-rays, and even to γ -rays over different timescales (e.g., Urry and Padovani 1995; Kollgaard 1994), which are commonly attributed to be synchrotron and inverse Compton radiation from plasma in a relativistic jet oriented at a small angle with our line of sight. As such, they represent a fortuitous natural laboratory to study the physics of jets, and ultimately the mechanisms of energy extraction from the central black holes, a fundamental goal of extragalactic astrophysics.

Earlier studies of BL Lac objects have shown that the systematic differences between radio and X-ray selected BL Lac objects (RBLs vs XBLs) are consistent with orientation differences (Kollgaard et al. 1996; Ghisellini et al. 1993). Meanwhile, BL Lac objects have been reclassified in a more physical way as “low energy” and “high energy” peaked BL Lac objects (LBLs vs HBLs) based on the peak frequency of synchrotron radiation (e.g. Giommi and Padovani 1994), rather than just observational selection. In general, RBLs and XBLs tend to be LBLs and HBLs, respectively. However, recent evidence has shown that some of the differences between HBLs and LBLs cannot be accounted for by differences in orientation alone (Sambruna, Maraschi & Urry 1996). The alternate explanation, that these classes are merely opposite extremes of the source’s spectral energy distribution (SED), also fails to explain some HBL-LBL differences (Kollgaard et al. 1996; Stocke 1996). Instead the modern thinking is that the HBL-LBL dichotomy represents two extremes of a continuum in either luminosity and viewing angle (Georganopoulos & Marscher 1998) or luminosity and peak frequency (Fossati et al. 1998).

Recent studies from deeper and larger X-ray surveys have indeed shown that BL Lac objects tend to exhibit more continuous distributions of properties (Sambruna et al. 1996; Scarpa and Falomo 1997; Perlman et al. 1998; Laurent-Muehleisen et al. 1999) rather than disparate ones. This has resulted in an important role for those objects with intermediate SEDs between HBL and LBL, namely intermediate BL Lac objects (IBLs), in revealing BL Lac mysteries.

In this paper, we present the X-ray spectral analysis (ROSAT and ASCA archival data) and the SED of a serendipitous BL Lac object, PKS 2316-423. It is a southern radio source at $z = 0.0549$, and was formerly classified as a BL Lac candidate on the base of its featureless non-thermal radio/optical continuum (Crawford & Fabian 1994; Padovani & Giommi 1996). We noticed this object as it has been the brightest con-

taminating source to the nearby narrow-line X-ray galaxy, NGC 7582 (Xue et al. 1998; Schachter et al. 1998) in most of its historical X-ray records.

The ROSAT(PSPC) and ASCA satellites observed this object as a serendipitous source in April 1993 and November 1994 respectively. These observations, though non-simultaneous, extend our knowledge of the source’s SED properties to the X-ray domain (0.1–10 keV), but also provide a good opportunity for X-ray spectroscopic studies, which turn out to be very important for its classification.

In section 2 we describe the observations and data reduction, and then present the spectral analysis in section 3. We construct the source SED in section 4 on the base of our newly X-ray flux measurements as well as the published photometry data. The results are summarized and discussed in section 5. Throughout this paper, $H_0 = 50 \text{ km s}^{-1}\text{Mpc}^{-1}$ and $q_0 = 0.5$ are assumed. All errors reported below are quoted at the 90% confidence level for one interesting parameter (i.e. $\Delta\chi^2 = 2.7$).

2. OBSERVATIONS AND DATA REDUCTION

To investigate the X-ray spectroscopic properties of PKS 2316-423, we collected the relevant data available in the NASA/GSFC data archive. This resulted in one ASCA, one ROSAT PSPC and two HRI pointed observations (see Table 1). All data were reduced using *XSELECT* within *FTOOLS* package version 4.2.

PKS 2316-423 is 17 arcmin away from the center of the ROSAT(PSPC) pointed observation, which was centered on NGC 7582. The source was somewhat affected by scattering and vignetting from the PSPC superstructure. We tried to extract the source counts using a larger chip region (with a radius as large as 3.2 arcmin) to account for former effect. The latter, which was estimated a $\sim 9\%$ effect at 1 keV, was corrected using a *FTOOLS*’s task, *pcarf*. The background was estimated from an annular source-free region. The source spectrum was also corrected for deadtime, and finally regrouped to at least 20 counts per channel. No significant variations in the source count rate were detected over the ~ 7200 -s ROSAT observation spanning a little more than one day.

Both the PKS 2316-423 and NGC 7582 were clearly detected in the ASCA observation with the two GIS and SIS instruments. The former instruments were operated in normal PH mode; the later were operated in 2 CCD mode (along the diagonal) and carefully oriented to place the two objects near the axis.

The ASCA data were selected from the intervals of high and medium telemetry rates for both GIS and SIS. The SIS data were screened using the following criteria: a) The data was not taken in the region of

the South Atlantic Anomaly, b) the angle between the field of view and the edge of the bright and dark earth exceeded 25° and 5° , respectively, and c) the cutoff rigidity was greater than $4 \text{ GeV } c^{-1}$. After these selections, we also deleted data if d) there were any spurious events or the dark frame error was abnormal. For GIS data, no bright earth angle and cutoff rigidity criteria were applied. More details concerning the performance and instrumentation of ASCA have been reported in separate papers (ASCA satellite: Tanaka et al. 1994; SIS: Burke et al. 1991; GIS: Ohashi et al. 1996).

Source counts of ASCA observation were extracted from circular regions of radius ~ 3 arcmin and ~ 5 arcmin for the SIS and GIS respectively. The background was extracted from the source free regions on the same detectors. No evident variations in the source count rate were detected either over the $\sim 19,000$ -s ASCA observation spanning about half a day.

3. SPECTRAL ANALYSIS

Since no evident variations in the source count rate were detected during either observations, the time-averaged spectra from both satellites were used for spectral analysis. The spectra of both ROSAT PSPC and ASCA were grouped so that each energy channel contains at least 20 counts allowing chi-squared minimization techniques. Spectral analysis have been performed using XSPEC(V10) program.³

3.1. The ROSAT Data

A simple power-law fit to the ROSAT PSPC data in the range of 0.1–2 keV gives photon index $\Gamma = 2.0 \pm 0.2$ and absorption column density of $(1.41 \pm 0.5) \times 10^{20} \text{ cm}^{-2}$ (Figure 1), which is consistent with the Galactic value $N_{\text{Hgal}} = 2.0 \times 10^{20} \text{ cm}^{-2}$ (Stark et al. 1992). This model describes the data reasonably well (Table 2). The fluxes corrected for the Galactic absorption are $4.20_{-0.28}^{+0.25} \times 10^{-12} \text{ ergs cm}^{-2} \text{ s}^{-1}$ in the 0.1–2.4 keV band and $1.83_{-0.12}^{+0.11} \times 10^{-12} \text{ ergs cm}^{-2} \text{ s}^{-1}$ in the 0.5–2 keV band, estimated from the best-fit power-law model. The inferred intrinsic luminosity is $5.7 \times 10^{43} \text{ ergs s}^{-1}$ in the 0.1–2.4 keV band, which is similar to that of other non-quasar AGN. The source was observed twice with ROSAT HRI in June 1992 and May 1993 respectively, the obtained count rates correspond to fluxes of $(5.9 \pm 0.3) \times 10^{-12} \text{ ergs cm}^{-2} \text{ s}^{-1}$ and $(6.1 \pm 0.3) \times 10^{-12} \text{ ergs cm}^{-2} \text{ s}^{-1}$ in the observed energy range 0.1– 2.4 keV, assuming a power-law spectrum identical to that of PSPC. The PSPC observation was made between the two HRI observations (Table 1), and recorded a relatively lower flux level. These factors suggest the source is

variable and thus there might be a non-thermal origin for the X-ray flux.

3.2. The ASCA Data

The spectra of the four ASCA instruments were fitted simultaneously in the range of 0.5–10 keV for SIS(0/1) and 0.7–10 keV for GIS(2/3). A simple power-law model gives an acceptable fit to the whole dataset (Table 2). However, comparing the results with the ROSAT data, the ASCA spectra suggest that the source spectral slope with photon index of $\Gamma = 2.4 \pm 0.2$ in the 0.5–10 keV broad-band is significantly steeper than that of ROSAT PSPC spectrum in the 0.1–2 keV band. In addition, the ASCA data requires an absorption column density of $8.8_{-5.3}^{+5.9} \times 10^{20} \text{ cm}^{-2}$ which is significantly in excess of the Galactic value. This is clear evidence of spectral variability, since the two observations were made 1.5 years apart. There are two possible explanations for this result: either a variable absorbing column (which, as described below, we believe to be unlikely), or a spectral flattening at soft energies due to a convex continuum. However, the first case seems unlikely, since that very few BL Lacs show evidence of significant cold absorbing gas in excess of line-of-sight Galactic column density (Perlman et al. 1996b; Urry et al. 1996). The recent detections of several BL Lacs by the Extreme Ultraviolet Explorer (EUVE) (Marshall, Fruscione, & Carone 1995; Fruscione 1996) is further evidence that these objects do not have significant intrinsic absorption.

For the latter case, the “excess” absorption seen in the ASCA spectrum might be an artifact falsely introduced in the fitting process. To test this idea, we next fitted the ASCA data using a broken power-law with a bound absorption at the Galactic value. Fitting with this model is notably improved ($\Delta\chi^2 = 6.8$ for two additional parameters, $P_F > 95\%$) compared to the fit of the single power-law model with the same bound absorption (Figure 2). The final fit yields two powerlaw components with a break-point at $\sim 2.1_{-0.7}^{+0.9}$ keV. The lower-energy component is flatter with a photon index of $\Gamma = 2.0_{-0.2}^{+0.4}$; the higher-energy component is steeper with $\Gamma = 2.6_{-0.3}^{+0.3}$. Thawing the absorption parameter in the broken power-law model produces little change of chi-squared value, and the resulted absorption column density is still consistent with the Galactic value (Table 3).

It should be noted that although the above two models cannot be statistically discerned, consider that the spectral-flattening effect is by far the more likely physical explanation of the ‘excess’ absorption seen in the ASCA spectra, hereafter, we would re-

³http://legacy.gsfc.nasa.gov/docs/xanadu/xspec/u_manual.html.

fer the broken power-law model as the best fit to the ASCA data.

Figure 3 shows confidence plots of the powerlaw spectral components versus the corresponding absorption column density for both the ASCA and ROSAT data. The ASCA observation described by the best-fitted model showed that the source brightness decreased by 33% in the 0.1–2.4 keV range compared with ROSAT PSPC data.

In summary, the ASCA observation of PKS 2316-423 in November 1994 is best-fitted by a broken power-law model, in which a relatively flatter component at lower energies below ~ 2.1 keV is very consistent with the shape of the ROSAT/PSPC spectrum observed in May 1993. This indicates that the broad-band X-ray spectral slope remained constant at lower-energies, even though the source brightness evidently decreased; however, the steeper component above ~ 2.1 keV does suggest the X-ray spectrum became softer at higher energies with the decreasing of the source brightness. As shown in the next section, the ROSAT and ASCA observations actually revealed a variable high-energy tail of the source synchrotron radiation.

4. SPECTRAL ENERGY DISTRIBUTION

The X-ray spectral analysis of PKS 2316-423 in the last section has shown its HBL-type properties. Moreover, even though non-simultaneous, the composite SED from the literature could present more insights on this object through comparison with the properties of the most recent complete BL Lac object samples. We plot in Figure 4 non-simultaneous radio, optical, UV and X-ray data, from both the space and ground-based observations, assuming an “average” SED of the source. It is clear that the composite SED from radio to X-ray is likely from only one radiation component (i.e., synchrotron emission). Its optical and ultraviolet radiation appear to be a continuation of the radio synchrotron spectrum; the X-ray data are likely from a common emission origin as the lower energy parts and represents a high energy tail of the synchrotron spectrum.

First, we derive some spectral parameters from the SED of PKS 2316-423. Following the general definition, we get the K-corrected two point spectral indices: radio-optical spectral index $\alpha_{ro} = 0.56$, optical-X-ray one $\alpha_{ox} = 1.18/1.26$ and radio-X-ray one $\alpha_{rx} = 0.78/0.82$ (note that hereafter the two values of one parameter is due to the different X-ray fluxes discussed in the last section). Because of the spectral variability shown evidently in the hard X-ray band (> 2 keV), the composite X-ray/optical

spectral, $\alpha_{xox} = \alpha_{ox} - \alpha_x$ also varied, with a value of 0.18/0.26 for $\alpha_x = 1.0^4$, and $\alpha_{xox} = -0.42/-0.34$ for $\alpha_x = 1.6$, respectively. Another important spectral parameter is the X-ray to radio logarithmic flux density ratio, and we get $\log S_X/S_r \sim -6.36/-6.29$.

Furthermore, it is clearly seen from Figure 4 that the radio to X-ray SED of PKS 2316-423 likely peaks in the EUV/soft-X-ray band. Following Sambruna et al. (1996), we performed a parabolic fit to the radio through optical/UV/X-ray SED of the source to determine the value of the peak frequency. We obtain $\nu_p = 7.3 \times 10^{15}$ Hz. The same fit yields an estimate of the luminosity at the peak frequency $L_p = 1.5 \times 10^{43}$ ergs s $^{-1}$ and of the integrated radio-to-X-ray synchrotron luminosity of $L_{syn} = 2.1 \times 10^{44}$ ergs s $^{-1}$. In the next section we will discuss the general SED properties of BL Lac objects and the attribute of PKS 2316-423.

For comparison, we plotted in Figure 4 the EGRET sensitivity threshold as an upper limit to the GeV flux (marked by an arrow), since the source was never detected at γ -rays. It is shown that the source is dominated by a synchrotron process in the a broad energy range below 10 keV; above which, we know nothing about the inverse-Compton emission which would undoubtedly dominate the source emission.

5. DISCUSSIONS

PKS 2316-423 was first serendipitously detected as a marginally extended (1.5 arcmin) X-ray source in the Einstein Medium-Sensitivity Survey (EMSS; Gioia et al. 1984; Stocke et al. 1991). The ROSAT HRI observation made by Crawford and Fabian (1994) in 1992 June confirmed the result of Einstein and further revealed a second weak X-ray source 10 arcsec (15 kpc) south of the galaxy which may be related to the central source. They suggested that PKS 2316-423 is a BL Lac object based on its probably non-thermal radio/optical/X-ray radiation, and has an “off-sight” jet component. If this is verified, then it will provide an interesting test case for both the host galaxies of BL Lac objects and their environment. Unfortunately, the later ROSAT HRI observation made in 1993 May did not go deep enough compared to the former observation, thus the misaligned scenario of this BL Lac object can hardly be further confirmed or constrained.

The multiple X-ray observations show that PKS 2316-423 was variable on timescales of weeks to years. The flux in the 0.1–2.4 keV band increased by ~ 50 % from ROSAT PSPC to HRI observations in a 13 day interval in May 1993, and dropped ~ 73 % 1.5 years later when observed with ASCA in November

⁴Note that the parameter used here refers to the energy spectral index, which is related to the photon spectral index with $\alpha_x = \Gamma - 1$.

1994. These factors suggest the source is variable and thus consistent with the expected characteristics of a high-energy tail from a dominant synchrotron emission. The source, however, did not show any short term variability during both ROSAT PSPC and ASCA observations spanned over ~ 1 day. More X-ray observations will be necessary.

X-ray spectral analysis provides more insights into the nature of the source's emission. A single power-law model fit to the ROSAT PSPC and ASCA data shows significant discrepancies. However, the two datasets can be reconciled if the ASCA spectrum is fit with a broken power-law model. This model indicates that, below an energy-break point, ~ 2.1 keV, there is a relatively flatter component ($\Gamma = 2.0^{+0.4}_{-0.2}$) to be consistent with the PSPC spectrum; and a steeper component with $\Gamma = 2.6^{+0.3}_{-0.3}$ above the energy-break point, this is one of the general X-ray spectral properties of a HBL (Sambruna et al. 1996). This kind of intrinsically downward curved X-ray spectrum can be easily interpreted as due to synchrotron losses from a relativistic plasma. The high-energy peaked SED of the source indicates that PKS 2316-423 is a HBL-type BL Lac object, with the X-ray spectrum being the high energy tail of synchrotron emission over a wide wavelength range, with correlated flux and spectral variability. With the decrease in source brightness from ROSAT PSPC to ASCA observations, the X-ray spectrum in 0.1–10 keV band became softer in the harder X-ray band.

The recent studies have greatly modified our view of BL Lac objects. DXRBS (Perlman et al. 1998), REX (Caccianiga et al. 1999), and RGB (Laurent-Muehleisen et al. 1999) surveys have shown that BL Lac objects exhibit a continuous distribution of properties rather than two distinct classes: HBLs vs LBLs (or XBLs vs RBLs). These findings show that the distribution of the SED parameters of BL Lac objects peaks where the empty region between the two extreme subclasses were previously seen. Therefore, most BL Lac objects should exhibit intermediate SED properties. The previously observed bimodal distribution is primarily due to observational selection effects (e.g. Laurent-Muehleisen et al. 1999).

Here we compare the SED properties of PKS 2316-423 with the general properties of BL Lacs found recently. When we put PKS 2316-423 ($\alpha_{ro} = 0.56$ and $\alpha_{ox} = 1.18/1.26$) on the α_{ro} vs α_{ox} color-color diagram, we find that it is a somewhat intermediate BL Lac object. As we know, α_{XOX} can more precisely measure spectral changes from optical to soft X-ray bands. If $\alpha_{XOX} \lesssim 0$, then the X-rays lie along a powerlaw or steepening synchrotron continuum. A positive value of α_{XOX} represents a concave spectrum and is likely caused by a hard inverse-Compton

component. The values of α_{XOX} for PKS 2316-423 depend on the X-ray spectral slopes in different variability states, being 0.18/0.26 and -0.42/-0.34 for $\alpha_x = 1.0$, in the high state of the ROSAT/PSPC observation, and 1.6, in the low state of the ASCA observation respectively. We find these values should just locate in the intermediate range of the α_{XOX} distribution of recent BL Lac samples (e.g., Perlman et al. 1998; Caccianiga et al. 1999; Laurent-Muehleisen et al. 1999). Interestingly, the value of α_{XOX} at different epoch was in opposite symbol, this might indicate that, in the different variability states of PKS 2316-423, the spectral change from optical to X-ray could show either synchrotron or inverse-Compton characteristics, just as would be expected for an IBL.

Previous studies show a clear bimodality in the ratio of the X-ray to radio flux densities of HBLs and LBLs at $\log S_X/S_r \sim -5.5$ (e.g. Padovani and Giommi 1995; Perlman et al. 1996a; Brinkmann et al. 1996). The value of $\log S_X/S_r$ for PKS 2316-423 is -6.36/-6.29, smaller than this sharp division value, seems in contradiction with its non-LBL attribute; however, the value is consistent with the distribution of the flux ratios of the intermediate BL Lacs found in DXRBS and RGB samples, which show no such dichotomy between HBL- and LBL-like SEDs (Perlman et al. 1998; Laurent-Muehleisen et al. 1999).

The importance of the frequency at which the synchrotron radiation peaks is that it provides a powerful diagnostic for the physical condition of the emitting region. Recent studies showed that among BL Lacs the synchrotron peak frequencies are inversely correlated with their luminosities (Fossati et al. 1998). Due to its low peak luminosity, PKS 2316-423 should be located near the bottom right end of Figure 7c of Fossati et al. (1998), with a peak frequency of around $\sim 10^{18}$ Hz. However the parabolic fit to the SED of PKS 2316-423 just gives $\nu_p \sim 10^{16}$ Hz. Consider the given ROSAT photon index of 2.0 (see section 3), which equates to a flat spectrum in νF_ν vs ν space within the soft X-ray range, suggesting that the peak frequency of PKS 2316-423 might be underestimated. This could be caused by imposing that the X-ray point smoothly connects to the lower energy data, as would happen in a parabolic fit. If a cubic fit is adopted, the synchrotron peak of PKS 2316-423 could be shifted toward a value of $\sim 10^{17}$ Hz, which is basically follows the general trend of inverse correlation of the synchrotron peak frequency versus the luminosity among blazars (Fossati et al. 1998). In this sense, however, the source also behaves like a typical HBL.

In summary, the averaged SED properties of PKS 2316-423 indicates that it is an IBL, like those many objects found in DXRBS (Perlman et al. 1998), REX

(Caccianiga et al. 1999) and RGB surveys (Laurent-Muehleisen et al. 1999). However, the source also shows some typical X-ray spectral properties of a HBL. This in fact supports a people's general idea – that in X-rays, an intermediate BL Lac object can show either synchrotron or inverse-Compton characteristics in different variability states. Though the most compelling test of the idea awaits a large sample of such studies.

We would like to thank the anonymous referee for his/her insightful comments that led to a number of significant improvements in this paper. This research has made use of the NASA/IPAC Extragalactic Database (NED) which is operated by the Jet Propulsion Laboratory, California Institute of Technology, under contract with the National Aeronautics and Space Administration. S.J.X. acknowledges the financial support from the Chinese Post-Doctoral Program.

REFERENCES

- Brinkmann, W., Siebert, J., Kollgaard, R.I., 1996, A&A, 313, 356
 Burke B.E., Mountain R.W., Harrison D.C., et al., 1991, IEEE Trans. ED-38, 1069
 Caccianiga, A., Maccacaro, T., Wolter, A. et al., 1999, ApJ, 513, 51
 Crawford C.S., Fabian A.C., 1994, MNRAS, 266, 669
 Fruscione, A., 1996, ApJ, 459, 509
 Fossati, G., Maraschi, L., Celloti, A. et al., 1998, MNRAS, 299, 433
 Georganopoulos, M., Marscher A.P., 1998, ApJ, 506, 621
 Ghisellini, G., Padovani, P., Celotti, A., Maraschi, L., 1993, ApJ, 407, 65
 Gioia I.M., Maccacaro T., Schild R.E. et al., 1984, ApJ, 283, 495
 Giommi P., Padovani P., 1994, MNRAS, 268, L51
 Kollgaard R.I., 1994, Vistas Astron., 38, 29
 Kollgaard R.I., Palma, C., Laurent-Muehleisen, S. A., Feigelson, E., 1996, ApJ, 465, 115
 Laurent-Muehleisen, S.A., Kollgaard, R.I., Feigelson, E. D., Brinkmann, W., Siebert, J., 1999, ApJ, 525, 127
 Marshall H.L., Fruscione, A., Carone T.E., 1995, ApJ, 439, 90
 Ohashi T., Ebisawa K., Fukazawa Y., et al. 1996, PASJ 48, 157
 Perlman, E.S., et al., 1996a, ApJS, 104, 251
 Perlman, E.S., Stocke, J.T., Wang, Q.D., Simon, L.M., 1996b, ApJ, 456, 451
 Perlman, E.S., Padovani, P., Giommi, P., 1998, AJ, 115, 1253
 Padovani P., Giommi P., 1995, ApJ, 444, 567
 Padovani P., Giommi P., 1996, MNRAS, 279, 526
 Sambruna, R.M., Maraschi, L., Urry, C.M., 1996, ApJ, 463, 444
 Scarpa, R. & Falomo, R., 1997 A&A 325, 109
 Schachter J.F., Fiore F., Elvis M., et al. 1998, ApJ, 503, L123
 Stark A.A., Gammie C.F., Wilson R.W. et al., 1992, ApJS, 79, 77
 Stocke J.T., Morris S.L., Gioia I.M., et al. 1991, ApJS, 76, 813
 Stocke J.T., 1996, Proc. IAU Symp. 175, New Observations of BL Lacertae Objects, eds. R.D. Ekers, C. Fanti & L. Padielli (Kluwer), 385
 Tanaka Y., Inoue H., Holt S.S. 1994, PASJ 46, L37
 Urry, C.M., Sambruna, R.M., Worrall, D.M. et al., 1996, ApJ, 463, 424
 Urry, C.M., Padovani P., 1995, PASP, 107, 803
 Xue S.J., Otani C., Mihara T. et al. 1998, PASJ, 50, 519

TABLE 1
 SUMMARY OF ROSAT AND ASCA DATA

Instrument	Date	Exposure (ksec)	Count rate (count s ⁻¹)
ROSAT PSPC	93/05/04	7.2	0.228 ± 0.006
ROSAT HRI	92/06/07	7.5	0.065 ± 0.003
ROSAT HRI	93/05/17	4.2	0.067 ± 0.004
ASCA SIS0	94/11/14	16.4	0.047 ± 0.002
ASCA SIS1		16.4	0.034 ± 0.002
ASCA GIS2		18.8	0.024 ± 0.002
ASCA GIS3		18.8	0.026 ± 0.002

TABLE 2
SIMPLE POWER-LAW FITS TO THE ROSAT PSPC AND ASCA DATA

Data	Γ	N_{H} (10^{20} cm^{-2})	$\chi^2_{\nu}/\text{d.o.f}$	$F_{1\text{keV}}^{\text{a}}$ ($10^{-12} \text{ ergs cm}^{-2} \text{ s}^{-1}$)	$F_{0.1-2\text{keV}}^{\text{a}}$ ($10^{-12} \text{ ergs cm}^{-2} \text{ s}^{-1}$)
ROSAT PSPC	$2.0^{+0.2}_{-0.2}$	$1.41^{+0.49}_{-0.43}$	1.1/17	$1.32^{+0.08}_{-0.09}$	$2.63^{+0.15}_{-0.18}$
ASCA	$2.4^{+0.2}_{-0.2}$	$8.78^{+5.97}_{-5.37}$	0.96/133	$1.10^{+0.16}_{-0.19}$	$1.35^{+0.33}_{-0.20}$

^aObserved fluxes (not corrected for absorption).

TABLE 3
BROKEN POWER-LAW FIT TO THE ASCA DATA

N_{H} (10^{20} cm^{-2})	Γ_1	E_{break} (keV)	Γ_2	$\chi^2_{\nu}/\text{d.o.f}$	$F_{0.5-2\text{keV}}^{\text{a}}$ ($10^{-12} \text{ ergs cm}^{-2} \text{ s}^{-1}$)	$F_{2-10\text{keV}}^{\text{a}}$ ($10^{-12} \text{ ergs cm}^{-2} \text{ s}^{-1}$)
$2.4^{+2.2}_{-2.0}$	$2.0^{+0.4}_{-0.2}$	$2.1^{+0.9}_{-0.7}$	$2.6^{+0.3}_{-0.3}$	0.95/131	$1.13^{+0.34}_{-0.16}$	$0.92^{+0.28}_{-0.14}$

^aObserved fluxes (not corrected for absorption).

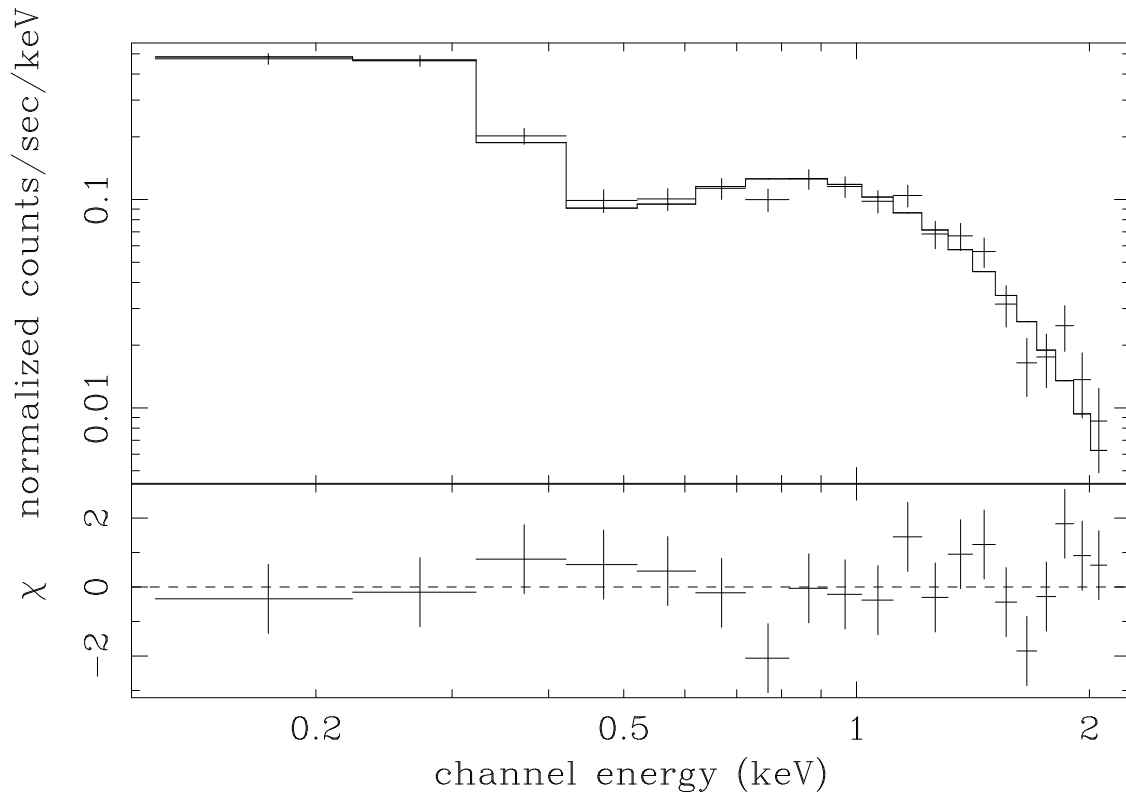


FIG. 1.— Folded ROSAT PSPC spectrum of PKS 2316-423 in May 1993. Single power-law fit to the observation and residuals are shown. The model gives acceptable fit to the data with an absorption in good agreement with the Galactic value.

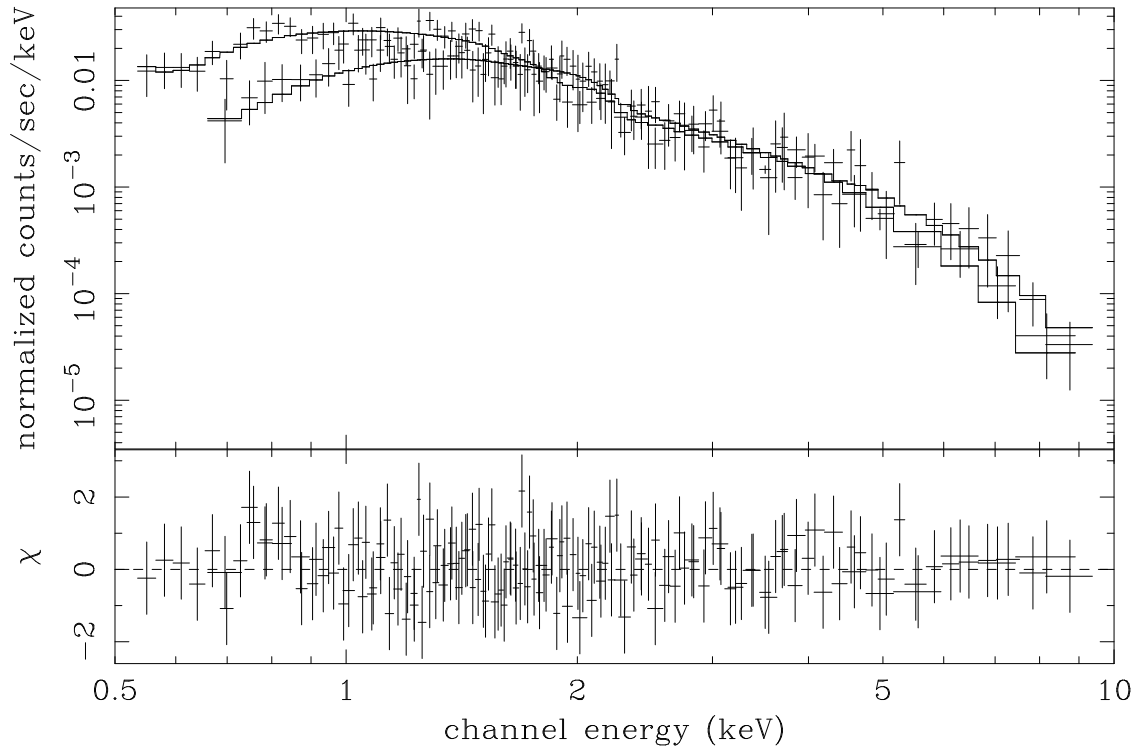


FIG. 2.— Folded ASCA spectra of PKS 2316-423 in November 1994. Data from all the four detectors were best fitted together with a broken power-law model (see text). Only combined SIS and GIS spectra are shown for conciseness.

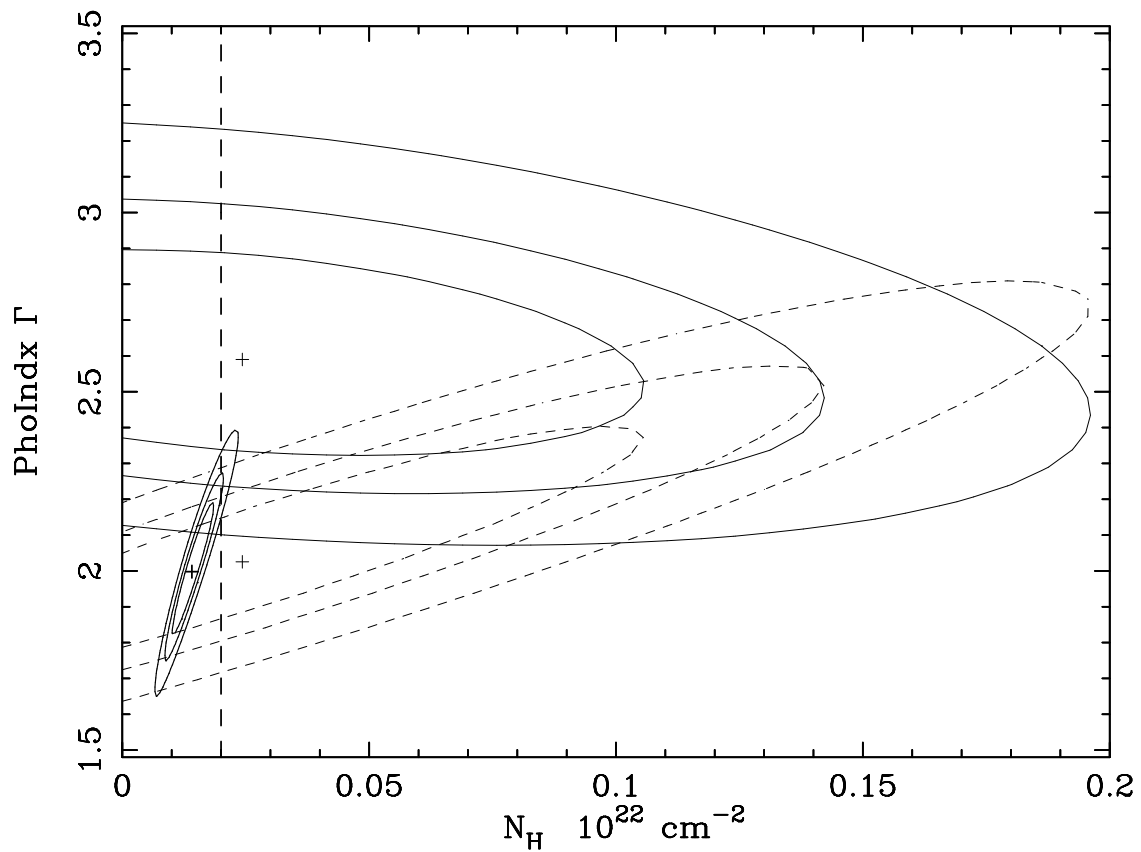


FIG. 3.— Confidence contour levels (68%, 90% and 99%) for the slope of power-law components vs. the absorption column density. The thin solid and dashed lines show the steep and flat components of the ASCA spectrum respectively. Thick solid lines show for the ROSAT/PSPC spectrum. The vertical dashed line shows the absorption column density at the Galactic value.

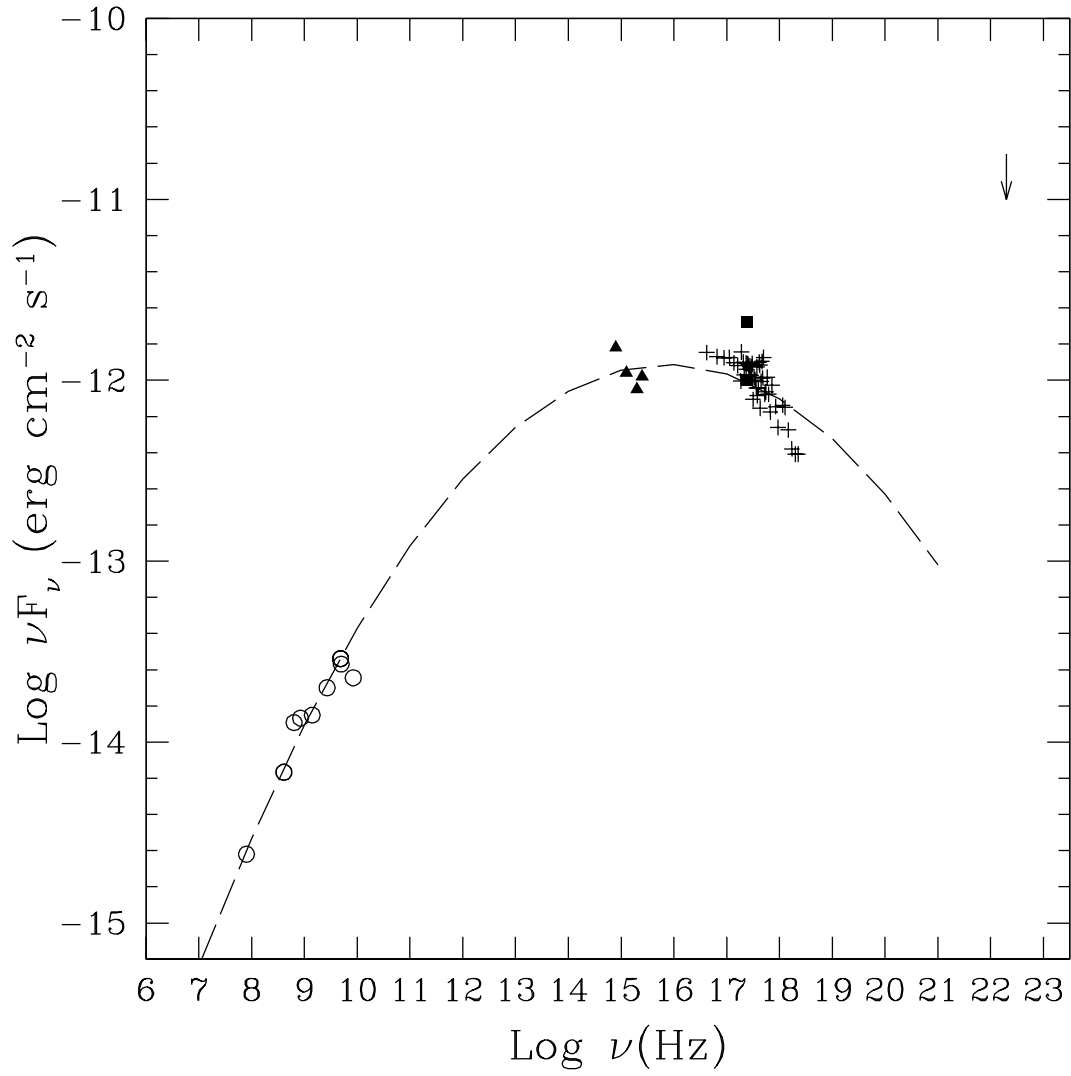


FIG. 4.— The multifrequency SED of PKS 2316-423 and its parabolic fit. The X-ray points are data from this paper, plotted with solid square for ROSAT/HRI and cross mark for ASCA and ROSAT/PSPC. The UV/optical points are data from Crawford and Fabian (1994) plotted with solid triangle. Circle symbols represent radio data from NASA/IPAC Extra-galactic Database (NED).